EXHIBITING PLANAR STRUCTURES FROM EGOMOTION

Samia Bouchafa, Antoine Patri and Bertrand Zavidovique
Institut d'Electronique Fondamentale, University Paris XI, 91405 Orsay Cedex, France

Keywords: Image motion analysis, Pattern recognition, Image scene analysis, Ego motion.

Abstract: This paper deals with plane extraction from a single moving camera through a new optical-flow cumulative process. We show how this c-velocity defined by analogy to the v-disparity in stereovision, could serve exhibiting any plane whatever their orientation. We focus on 3D-planar structures like obstacles, road or buildings. A translational camera motion being assumed, the c-velocity space is then a velocity cumulative frame in which planar surfaces are transformed into lines, straight or parabolic. We show in the paper how this representation makes plane extraction robust and efficient despite the poor quality of classical optical flow.

1 INTRODUCTION

Our work deals with obstacle detection from moving cameras. In this application, most of real-time implemented approaches are based on stereovision. Yet stereo analysis shows two main drawbacks. First, it tends to group objects which are close to one-an-other. Second, height thresholds limit the detection implying to miss small obstacles close to the ground for example. Motion information is only exploited afterwards for detected objects. Motion analysis, on the other hand, allows the detection of any moving object. Therefore, we propose to exploit the ego-motion of the camera to distinguish between various moving objects. To that aim, we have established a correspondence with a very efficient stereovision technique based on the **v**-disparity concept (Labayrade, Aubert and Tarel, 2002). Our conjecture is that such result is general. Thereby we show how to extend the technique to detect planes along an image sequence shot from a moving vehicle. The apparent velocity from the scale change occurring to image data takes place of the disparity leading to the so-called **c**-*velocity* frame. In this paper we propose a complete plane detection process. Peculiar emphasis is placed on the parabolas detection in the **c**-*velocity* space.

The paper is organized as follows: in the next section we take a look at ego-motion based object detection. Then we recall some pertaining relations between 2D and 3D motion. The fourth part is devoted to the computation of constant velocity curves in the image plane – analogue in our ***c**-velocity* frame of the lines of the *v-disparity*, and we explain the cumulative process. The fifth section details how parabolas – 3D planes – are extracted in the ***c**-velocity* space using a Hough transform enriched by a K-mean technique. After the section devoted to results we conclude with discussions and future work.

2 PREVIOUS WORK

Recent years have seen a profusion of work on 3D motion, ego-motion or structure from motion estimation using a moving camera. It was followed by numerous classifications of existing methods based on various criteria. A classification commonly accepted groups existing techniques into three main categories: discrete, continuous and direct approaches.

- Discrete approaches (Hartley, 1995) are based on matching and tracking primitives that are extracted from image sequences (point, contour lines, corners, etc.). They are usually very effective. However, they suffer from a lack of truly reliable and stable features, e.g. time and viewpoint invariant. Moreover, in applications where the camera is mounted on a moving vehicle, homogeneous zones or linear marking on the ground hamper the extraction of reliable primitives.

Bouchafa S., Patri A. and Zavidovique B. (2009).
EXHIBITING PLANAR STRUCTURES FROM EGOMOTION.
In *Proceedings of the 6th International Conference on Informatics in Control, Automation and Robotics - Robotics and Automation*, pages 183-188
DOI: 10.5220/0002194601830188

- Continuous approaches exploit optical flow (MacLean, Jepson and Frecker, 1994). The relationship between the computed optical flow and real theoretical 3D motion allows - through optimization techniques - to estimate the motion parameters and depth at each point. Results are dependent on the quality of the computed optical flow.

- In direct approaches (Stein, Mano and Shashua, 2000), motion is determined directly from the brightness invariance constraint without having to calculate explicitly an optical flow. Motion parameters are then deduced by conventional optimization approaches.

- A large group of approaches (Irani, Rousso and Peleg, 1997) - which can be indifferently discrete, continuous or direct - exploits the parallax generated by motion (motion parallax, affine motion parallax, plane+parallax). These methods are based on the fact that depth discontinuities make it doable to separate camera rotation from translation. For instance, in "Plane+parallax" approaches, knowing the 2D motion of an image region where variations in depth are not significant permits to eliminate the camera rotation. Using the obtained residual motion parallax, translation can be exhibited easily.

3 PRELIMINARIES

Consider a coordinate system O XYZ at the optical centre of a pinhole camera, such that the axis OZ coincides with the optical axis. We assume a translational rigid straight move of the camera in the Z direction. That does not restrict the generality of computations. Moreover, the origin of the image coordinates system is placed on the top left of the image. If (x_0, y_0) are the coordinates of the principal point, then the ego-motion (u, v) becomes:

$$u = \frac{T_z}{Z}\left(y_0 - y\right) \text{ and } v = \frac{T_z}{Z}\left(x - x_0\right)$$

The previous equations describe a 2D motion field that should not be confused with optical flow which describes the motion of observed brightness patterns. We will assume here that optical flow is a rough approximation of this 2D motion field. In order to tackle the imprecision of optical flow velocity vectors, we propose to define a Hough-like projection space which – thanks to its cumulative nature –allows performing robust plane detection.

4 NEW CONCEPT: C-VELOCITY

In stereovision, along a line of a stereo pair of rectified images, the disparity is constant and varies linearly over a horizontal plane in function of the depth. Then, in considering the mode of the 2-D histogram of disparity value vs. line index, i.e. the so called *v-disparity* frame, the features of the straight line of modes indicate the road plane for instance (Labayrade, Aubert and Tarel, 2002). The computation was then generalized to the other image coordinate and vertical planes using the *u-disparity* by several teams including ours on our autonomous car.

In the same way we have transposed this concept to motion. Our computations build on the fact that any move of a camera results into an apparent shift of pixels between images: that is disparity for a stereo pair and velocity for an image sequence. The *v-disparity* space draws its justification, after image rectification that preserves horizontal – iso-disparity – lines, from inverse-proportional relations between first image horizontal-line positions vs. depth, second depth vs. disparity. We show here under how to exhibit the same type of relation in the ego-motion case between $\|\mathbf{w}\|$ (≅ disparity) and the iso-velocity function index *c* (≅ line index *v*).

$$\|\mathbf{w}\| = \sqrt{u^2 + v^2} = \left|\frac{T_z}{Z}\right| \sqrt{(y_0 - y)^2 + (x - x_0)^2}$$

$$\|\mathbf{w}\| = K \times f(x, y) \Rightarrow \frac{\|\mathbf{w}\|}{K} = f(x, y) = c$$

The translation T_Z being that of the camera, identical for all static points, if depth *Z* is constant the iso-velocity curves are circles. *c* varies linearly with the velocity vector. Beyond that “punctual” general case, *Z* can be eliminated in considering linear relations with (*X*,*Y*) i.e. plane surfaces well fitting the driving application for instance.

4.1 The Case of a Moving Plane

Suppose now the camera is observing a planar surface of equation (Trucco and Poggio, 1989): $\mathbf{n}^{\mathrm{T}}\mathbf{P} = d$, with $\mathbf{n} = (n_x, n_y, n_z)$ the unit normal to the plane and *d* the distance "plane to origin". Let us assume that the camera has a translational motion $\mathbf{T} = \left(0, 0, T_Z\right)$. We study four pertaining cases of moving planes and establish the corresponding motion field. a) Horizontal: road. b) Lateral: buildings. c)Frontal$_1$: fleeing or approaching obstacle, with $\mathbf{T} = (0, 0, T_Z^o)$. d) Frontal$_2$: crossing obstacle, with $\mathbf{T} = (T_X^o, 0, 0)$.

	Normal vector	*Associated 3D motion*	*Dist. to the origin*
a)	$\mathbf{n} = (0,1,0)$	$\mathbf{T} = \left(0, 0, T_Z\right)$	dist. d_r
b)	$\mathbf{n} = (1,0,0)$	$\mathbf{T} = \left(0, 0, T_Z\right)$	dist. d_b
c)	$\mathbf{n} = (0,0,1)$	$\mathbf{T} = \left(0, 0, T_Z + T_Z^o\right)$	dist. d_o
d)	$\mathbf{n} = (0,0,1)$	$\mathbf{T} = \left(T_X^o, 0, T_Z\right)$	dist. d_o

The corresponding motion fields, after [2] for instance, become those listed in the table below for each case. Let $\|\mathbf{w_o}\|$, $\|\mathbf{w_r}\|$ and $\|\mathbf{w_b}\|$ be respectively the module of the apparent velocity of an obstacle point, a road point and a building point. We choose to group all extrinsic and intrinsic parameters in a factor *K* and make it the unknown:

a)	$u = \frac{T_Z}{f \times d_r}(y - y_0)(x_0 - x)$ $v = \frac{T_Z}{f \times d_r}(x_0 - x)^2$
b)	$u = \frac{T_Z}{f \times d_b}(y - y_0)^2$ $v = \frac{T_Z}{f \times d_b}(y - y_0)(x_0 - x)$
c)	$u = \frac{T_Z + T_Z^o}{d_o}(y - y_0)$ $v = \frac{T_Z + T_Z^o}{d_o}(x_0 - x)$
d)	$u = \frac{T_Z}{d_o}(y - y_0) - \frac{T_X^o f}{d_o}$ $v = \frac{T_Z}{d_o}(x_0 - x)$

a)	$\|\mathbf{w}_r\| = K\sqrt{(x_0 - x)^4 + (y - y_0)^2 (x_0 - x)^2}$
b)	$\|\mathbf{w}_r\| = K\sqrt{(y - y_0)^4 + (y - y_0)^2 (x_0 - x)^2}$
c)	$\|\mathbf{w}_r\| = K\sqrt{(y - y_0)^2 + (x_0 - x)^2}$
d)	$\|\mathbf{w}_o\| = K$ if T_X^o □ $\mathrm{T_Z}$ $\|\mathbf{w}_o\| = K\sqrt{(x_0 - x)^2 + (y - y_0)^2}$ otherwise

Each type of $\|\mathbf{w}\|$ leads to the corresponding expression of **c** and then to the related iso-velocity curve. For instance in the case of a building plane:

$$c = \frac{\|\mathbf{w}\|}{K} = \sqrt{(y - y_0)^4 + (y - y_0)^2 + (x_0 - x)^2}$$

The final formula above proves that *c* is constant along iso-velocity curves and proportional to $\|\mathbf{w}\|$**,** same as the disparity is proportional to the line value *v*. Thus, as explained in introduction, the **c**-*velocity* space will be a cumulative space that is constructed in assigning to each pixel (x, y) the corresponding *c* value through the chosen model, and in incrementing the resulting $\left(c, \|\mathbf{w}\|\right)$ cell were **w** is the velocity found in (x, y). The latter **w** is computed thanks to a classical optical flow method. A study of the function $c(x, y)$ that corresponds to each plane model – in particular for the road and the building model – led us to the following conclusions: first, each previous curve intersects the *x* axis (road model) or *y* axis (building model) in the image plane in: $y_0 \pm \sqrt{c}$ or $x_0 \pm \sqrt{c}$ respectively. Second, for a standard image size, the range of variation of *c* is very large. For instance, for an image size of 320×240: $c_{\max} = 32000$ (road model) and 24000 (building model). As a consequence and for implementation reasons, we propose to deal for these two models with the relations between ||**w**|| and $\sqrt{c}$ (see Figure 1).

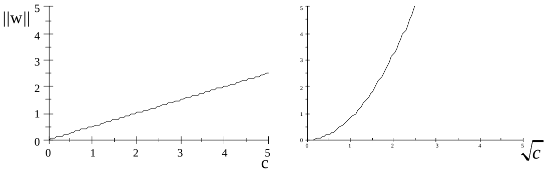

Figure 1: The c-velocity space that depends on the chosen relation between c and w: Linear for the obstacle model and parabolic for the road and the building model.

4.2 Cumulative Curves

For each point $\mathbf{p} = (x, y)$ in the image, there is an associated **c** value depending on the chosen plane model (see left column of Figure 2). We can calculate it once off-line because it only depends on (x, y). Also, it is possible for implementation facilities and by analogy to image rectification (that makes all epipolar lines parallel) to compute the transformation that makes all the c-curves parallel to the image line, that is the intensity function $I(c,y)$ for road and obstacle model and $I(x,c)$ for building model (see right column of Figure 2).

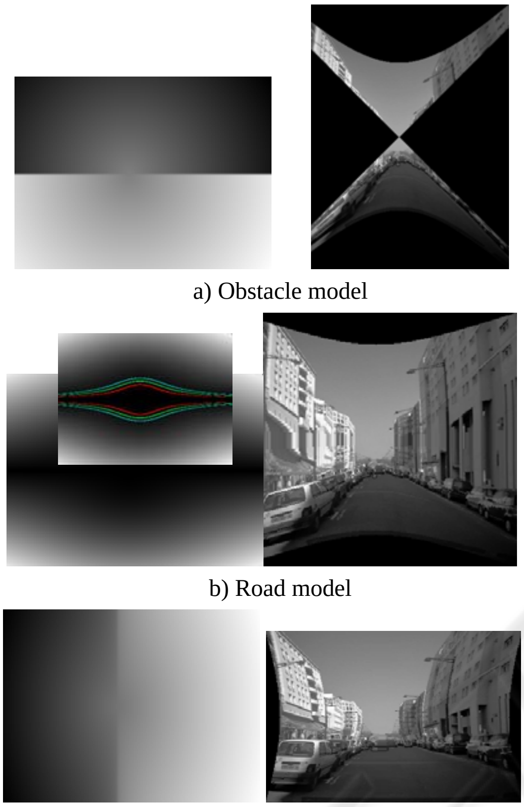

a) Obstacle model

b) Road model

c) Building model

Figure 2: Left: for each model, the corresponding c-values for each point of the image. Right: images constructed using the geometric transformation that makes all c-curves parallel**.**

5 1D HOUGH TRANSFORM AND K-MEAN CLUSTERING FOR PARABOLAS EXTRACTION

Planes are represented in the **c**-*velocity* space by parabolas that could be extracted using a Hough transform. The distance *p* between each parabola and its focus or its linea directrix is then cumulated in a one dimensional Hough transform (see Figure 3). The classes of the histogram split by K-mean clustering. Of course, any other clustering approach could be applied.

$$\|w\| = K\left(\sqrt{c}\right)^2 \Rightarrow p = -\frac{1}{4K} = -\frac{\left(\sqrt{c}\right)^2}{4\|w\|}$$

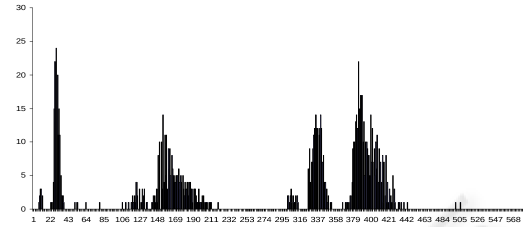

Figure 3: Example of a 1D Hough transform on the c-velocity space for detecting parabolas. For each (c,w) cell, a *p* value is cumulated.

6 EXPERIMENTAL RESULTS

In Figure 4, we have considered an image sequence in which one can see 6 moving planes: 2 planes corresponding to buildings, 2 planes corresponding to cars parked on the sides, a frontal moving obstacle (a motorcycle crossing the road) and the road plane. We have used the Lukas & Kanade method for optical flow estimation (Lucas and Kanade, 1981). In this sequence, velocity vectors are in majority on vertical planes. In the building **c**-velocity space, we get as expected 4 parabolas (see Figure 4.b). We have studied in the effects of 3 kinds of perturbations that have a consequence on the thickness of the parabolas. First, inter-model perturbation, second the imprecision on optical flow and third the possible pitch, yaw or roll of the camera. We use 2 kinds of confidence factors. First one is related to the translational motion hypothesis; it is the difference Δ_{foe} between the coordinate of image centre and the position of the Focus of expansion (for its estimation see section 6.1, results on Figure 6). Second one is related to possible contamination by planes of other models; it is the variance σ of each K-mean class. Points far from the mean belong probably to another plane model (Figure 4.c).

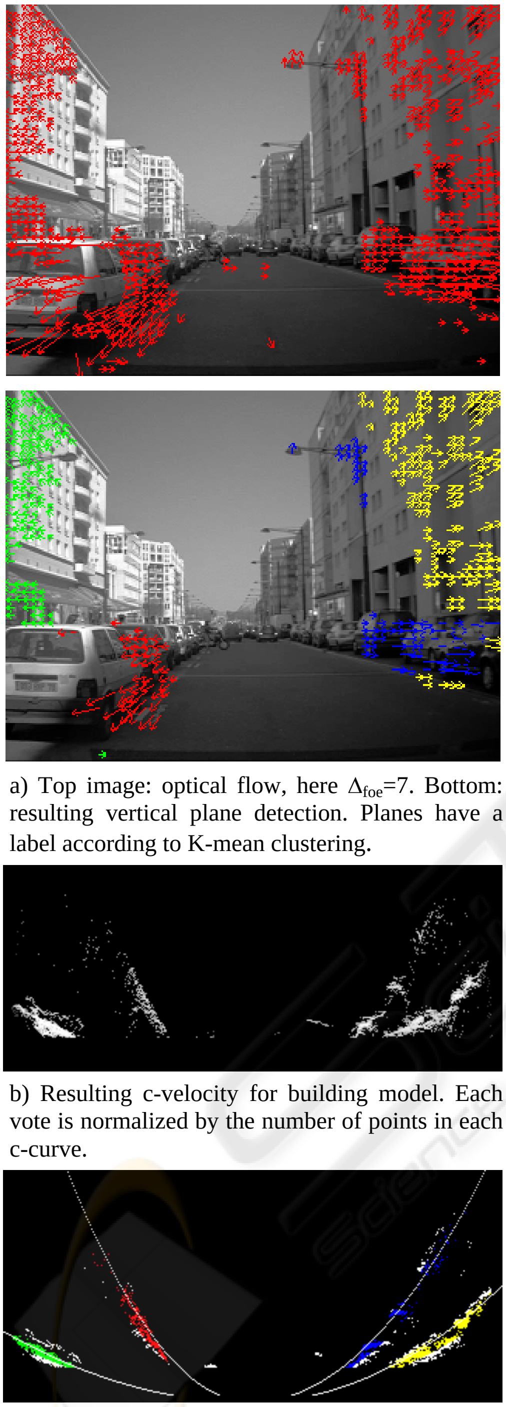

a) Top image: optical flow, here Δ_{foe}=7. Bottom: resulting vertical plane detection. Planes have a label according to K-mean clustering.

b) Resulting c-velocity for building model. Each vote is normalized by the number of points in each c-curve.

c) Results of parabolas extraction using a 1D Hough transform followed by a K-mean clustering (4 classes). In white the points that are discarded: they probably belong to another plane model. σ_{mean} = 10.

Figure 4: Example of results obtained from a database of the French project "Love" (Logiciel d'Observation des VulnérablEs).

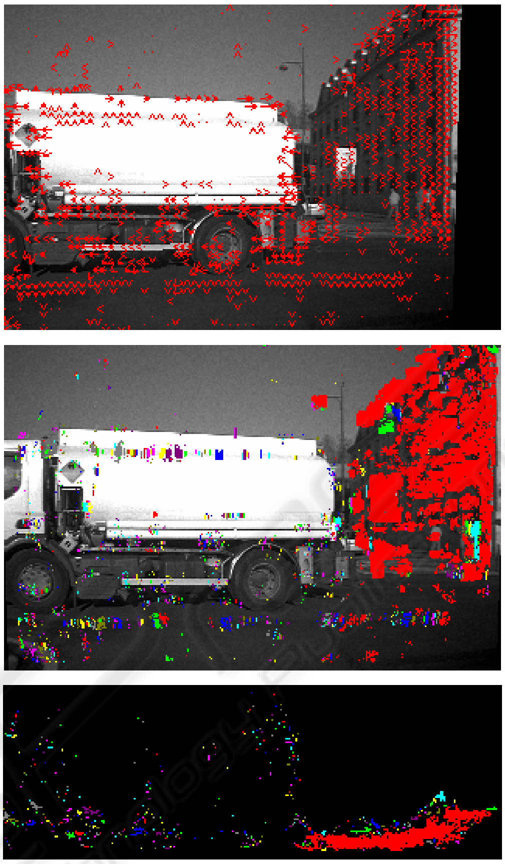

Figure 5: Results of a building detection (top left image in red). The crossing obstacle here is – as expected – not detected in the building **c**-*velocity* space.

6.1 FOE Estimation

Several methods exist (Sazbon, Rotstein and Rivlin, 2004). For sake of further real on board implementation, we favor here a method coherent with the present computations. All pixels are asked to vote for a global intersection point of apparent velocity vectors within a regular Hough space.

Indeed, in the case of a translational motion, each velocity vector with angle θ is directed toward the FOE. Let us assume that (x_0, y_0) are the FOE coordinates in the image. Then we have:

$$\theta = \tan^{-1}\left(\frac{v}{u}\right) = \tan^{-1}\left(\frac{x - x_0}{y_0 - y}\right)$$

The above relation means that we can extract the FOE by estimating the intersection of all velocity vector lines. In practice, we have carried out a voting space where each velocity vector votes for all the points belonging to its support line. The FOE corresponds then to the point with maximum votes.

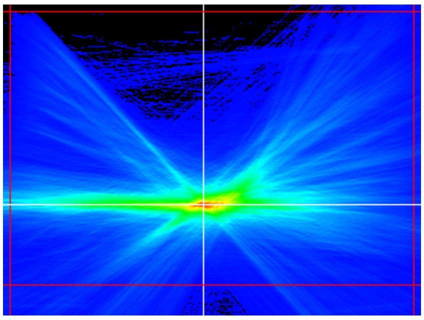

Figure 6: Voting space for FOE determination.

6.2 Results on Synthetic Images

In the following toy example, we generate a synthetic velocity vectors field of a moving 3D scene with 3 planes: a vertical one (on the left of the image), an horizontal one (on the bottom of the image) and a frontal plane with its own motion parameters (a crossing obstacle), see Figure 7.a.

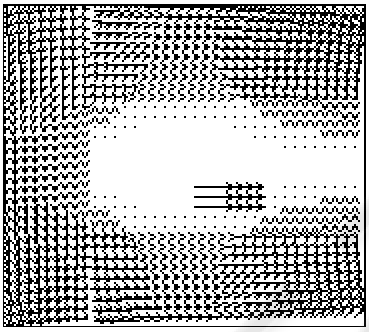

a) Velocity vectors field of a moving scene with a building, a road and an obstacle plane.

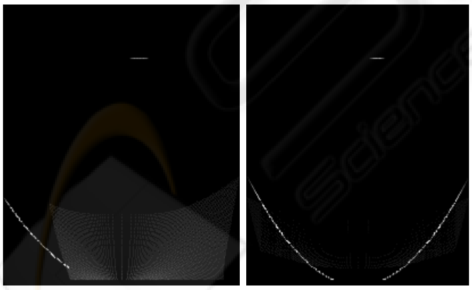

b) Associated c-velocity spaces (left: building, right: road). The parabolas indicate the expected moving planes. The constant segment corresponds to the obstacle; it appears in all the c-velocity spaces because of its constant velocity.

Figure 7: Results on synthetic images.

The results confirm that this simulated ego-motion (Figure 7,b) transforms a road plane and a building plane into a parabola in the corresponding c-velocity space. Likewise the obstacle in the middle of the road is a segment with its own constant **w.**

7 CONCLUSIONS

First results are very encouraging and confirm that the cumulative process is efficient in retrieving major entities of a moving scene environment. Our future work deals with implementing an iterative approach that deals with all the c-velocity spaces. Each detected plane from a given space could be discarded from the other spaces in order to reduce inter-model perturbation. On the other hand, we propose to progressively generalize the approach to more complex structures than planes and to more complex motion models, including rotations for instance.

REFERENCES

Hartley, R.I, 1995. In defense of the 8-point algorithm. In Proc. *IEEE Int. Conf. on Computer Vision*, Cambridge, MA, pp. 1064-1070.

Irani, M , Rousso, B, Peleg, S, 1997. Recovery of Ego-Motion using region alignment. In *IEEE Trans on PAMI*, vol. 19, n°3.

Labayrade, R, Aubert, D, Tarel, JP, 2002. Real Time Obstacle Detection on Non Flat Road Geometry through 'V-Disparity' Representation. In *IEEE Intelligent Vehicles Symposium 2002*, Versailles, June 2002.

Lucas, B.D, Kanade, T, 1981. An Iterative Image Registration Technique with an Application to Stereo Vision (DARPA). In *Proceedings of the 1981 DARPA Image Understanding Workshop*, pp. 121-130.

MacLean, W.J, Jepson, A.D , Frecker, R.C, 1994. Recovery of egomotion and segmentation of independant object motion using the EM algorithme. In *Proc. of the 5th British Machine Vision Conference*, pp. 13-16, York, U. K.

Sazbon, D, Rotstein, H, Rivlin, E, 2004. Finding the focus of expansion and estimating range using optical flow images and a matched filter. In *MVA*, vol. 15, n°4, pp. 229-236.

Stein, G. P , Mano, O, Shashua, A, 2000. A robust method for computing vehicle ego-motion. In *IEEE Intelligent Vehicles Symposium*, Dearborn, MI.

Trucco, E, Poggio, T, 1989. Motion field and optical flow: qualitative properties. In *IEEE Transactions on Pattern Analysis Machine Intelligence*, vol. 11, pp. 490-498.